

Quantifying the hip-ankle synergy in short-term maximal cycling

BURNIE, L., BARRATT, P., DAVIDS, Keith <<http://orcid.org/0000-0003-1398-6123>>, WORSFOLD, P. and WHEAT, Jonathan <<http://orcid.org/0000-0002-1107-6452>>

Available from Sheffield Hallam University Research Archive (SHURA) at:

<https://shura.shu.ac.uk/30710/>

This document is the Accepted Version [AM]

Citation:

BURNIE, L., BARRATT, P., DAVIDS, Keith, WORSFOLD, P. and WHEAT, Jonathan (2022). Quantifying the hip-ankle synergy in short-term maximal cycling. *Journal of Biomechanics*, 142, p. 111268. [Article]

Copyright and re-use policy

See <http://shura.shu.ac.uk/information.html>

1 **Quantifying the hip-ankle synergy in short-term maximal cycling**

2 Louise Burnie^{1,2,3*}; Paul Barratt⁴; Keith Davids²; Paul Worsfold^{3,5}; Jon Wheat⁶.

3 ¹*Department of Sport, Exercise and Rehabilitation, Faculty of Health and Life Sciences,*

4 *Northumbria University, Newcastle upon Tyne, UK*

5 ²*Sport and Physical Activity Research Centre, Sheffield Hallam University, Sheffield, UK*

6 ³*Biomechanics, English Institute of Sport, Manchester, UK*

7 ⁴*BAE Systems Digital, Manchester, UK*

8 ⁵*Sport and Exercise Sciences, University of Chester, Chester, UK*

9 ⁶*College of Health, Wellbeing and Life Sciences, Sheffield Hallam University, Sheffield, UK*

10 *Corresponding author – Louise Burnie. E-mail: louise.burnie@northumbria.ac.uk

11 T: (+44) 7801896584

12

Abstract

Simulation studies have demonstrated that hip and ankle joints form a task-specific synergy during downstrokes in maximal cycling to enable power produced by hip extensor muscles to be transferred to the crank. Existence of the hip-ankle synergy has not been investigated experimentally. Therefore, we sought to apply a modified vector coding technique to quantify the strength of the hip-ankle moment synergy in the downstroke during short-term maximal cycling at a pedalling rate of 135 rpm. Twelve track sprint cyclists performed 3 x 4 s seated sprints at 135 rpm. Joint moments were calculated via inverse dynamics, using pedal forces and limb kinematics. The hip-ankle moment synergy was quantified using a modified vector coding method. Results showed, for 28.8% of the downstroke, hip and ankle moments were in-phase, demonstrating the hip and ankle joints tend to work in synergy in the downstroke, supporting findings from simulation studies of cycling. At a pedalling rate of 135 rpm the hip-phase was most frequent (42.5%), significantly differing from the in- ($P = 0.044$), anti- ($P < 0.001$), and ankle-phases ($P = 0.004$), demonstrating hip-dominant action. Our results experimentally confirm the hip-ankle synergy, indicating an important mechanism that allows production of crank power during maximal sprint cycling.

Keywords: joint moments, movement coordination, sprint cycling, vector coding.

1 Introduction

The goal of short-term maximal cycling is to maximise mechanical power output delivered to the crank (van Soest & Casius, 2000). To achieve this, muscle and joint actions need to be coordinated to facilitate energy transfer from muscles through body segments to deliver maximum effective crank force (Raasch et al., 1997). Uni-articular hip and knee extensor muscles (gluteus maximus and vastii) are the primary power producers in maximal cycling

(Dorel et al., 2012; Martin & Nichols, 2018; Raasch et al., 1997; van Ingen Schenau et al., 1992). Simulation studies have demonstrated that hip extensor muscles (gluteus maximus) produce energy in the downstroke, transferred to the limb (Fregly & Zajac, 1996; Raasch et al., 1997). Additionally, ankle plantar-flexor muscles (gastrocnemius and soleus) need to be co-excited with hip extensors to form a synergy to transfer this energy to the crank (Dorel et al., 2012; Raasch et al., 1997). Without this co-excitation, simulations indicate that energy produced by hip extensors would simply accelerate limbs (dorsiflexing the ankle and hyperextending the knee), rather than being transferred into effective crank force (Raasch et al., 1997). Knee extensors (vastii) are able to transfer most of the energy they generate directly to the crank (Raasch et al., 1997). Martin and Nichols (2018) provided further evidence for this functional coordination mechanism using simulated work loops. They demonstrated that the ankle has a different role to knee and hip joints in maximal cycling - acting to transfer - instead of maximising muscle power (Martin & Nichols, 2018). However, existence of the hip-ankle synergy has not been verified experimentally. Hence, developing a method to experimentally quantify the strength of this synergy in cycling performance is important.

Vector coding can be used to quantify inter-segment, inter-joint and inter-limb coordination (Bayne, 2020; Chang et al., 2008; Hamill et al., 2000; Wheat & Glazier, 2006). It has been used to quantify inter-segment coordination between experienced and less experienced runners (Hafer et al., 2019), anticipated and unanticipated sidestepping (Weir et al., 2019) and during gait (Chang et al., 2008; Needham et al., 2014). Vector coding can identify and quantify coordination differences between-participants and movements, providing insights into coordination patterns not evident from joint or segment angle data alone (Needham et al., 2014; Wheat & Glazier, 2006). Vector coding of joint moment data could provide a useful

methodology to quantify strength of hip-ankle joint moment synergies in short-term maximal cycling.

This study aimed to apply a vector coding technique to quantify strength of hip-ankle moment synergies in downstrokes during short-term maximal cycling at a pedalling rate of 135 rpm.

2 Methods

2.1 Participants

Twelve, competitively-experienced, track sprint cyclists, at U-23 international level (n=5), Master's international and national levels (n=4), or Junior national level (n=3) participated in this study. Participants were varied in sex, age and anthropometrics (4 males and 8 females, age: 24.1 ± 13.8 yr, body mass: 68.2 ± 11.1 kg, height: 1.70 ± 0.07 m), and were similar in cycling performance level (flying 200 m personal best: 11.61 ± 0.90 s). Participants were provided with study details and gave written informed consent. The study was approved by the Sheffield Hallam University Research Ethics Committee.

2.2 Experimental protocol

An isokinetic ergometer was set up to replicate each participant's track bicycle position. Riders undertook their typical warm-up on the ergometer at self-selected pedalling rates and resistance for at least 10 minutes, followed by one 4 s familiarisation sprint at 135 rpm. Riders then undertook 3 x 4 s seated sprints at 135 rpm with 4 minutes recovery between efforts. A pedalling rate of 135 rpm was chosen as this is representative of the pedalling rate during the flying 200 m event in track cycling and within an optimal pedalling rate range for track sprint cyclists (Dorel et al., 2005; Kordi et al., 2020).

Isokinetic ergometer

A SRM cycle ergometer frame and flywheel (Julich, Germany) were used to construct an isokinetic ergometer (Burnie et al., 2020). The modified ergometer flywheel was driven by a 2.2-kW AC induction motor (ABB Ltd, Warrington, UK), controlled by a frequency inverter equipped with a braking resistor (Model: Altivar ATV312 HU22, Schneider Electric Ltd, London, UK) (Burnie et al., 2020). This set-up enabled participants to start their bouts at the target pedalling rate, rather than expending energy in accelerating the flywheel. The ergometer was fitted with force pedals (Model ICS4, Sensix, Poitiers, France) and a crank encoder (Model LM13, RLS, Komenda, Slovenia), sampling data at 200 Hz.

2.3 Kinematic and kinetic data acquisition

Two-dimensional kinematic data of each participant's left side were recorded at 100 Hz using one high speed video camera with infra-red ring lights (Model: UI-522xRE-M, IDS, Obersulm, Germany) (Burnie et al., 2020). Reflective markers were placed on the pedal spindle, lateral malleolus, lateral femoral condyle and greater trochanter. Kinematics and kinetics on the ergometer were recorded by CrankCam software (CSER, SHU, Sheffield, UK), which synchronised the camera and pedal force data and was used for data processing (Burnie et al., 2020).

2.4 Data processing

All kinetic and kinematic data were filtered using a Butterworth fourth order (zero lag) low pass filter, with a cut off frequency of 14 Hz. Instantaneous left crank power was calculated from the product of the left crank torque and crank angular velocity. The average left crank power was calculated by averaging the instantaneous left crank power over a complete pedal revolution. Joint moments were calculated via inverse dynamics (Elftman, 1939), using pedal

forces, limb kinematics, and body segment parameters (de Leva, 1996). Joint extension moments were defined as positive.

Data were analysed using a custom Matlab (R2017a, MathWorks, Cambridge, UK) script. Each sprint lasted for 4 s, revealing six complete crank revolutions. Joint moments were resampled to 100 data points around the crank cycle and the mean value at each time point was calculated to obtain a single, ensemble-averaged time series for each trial. Owing to technical problems for two participants only data from two instead of three sprints were collected.

Quantifying hip-ankle joint synergy

To quantify hip-ankle joint coordination and strength of hip-ankle joint synergies a vector coding method was applied to joint moment-moment diagrams (Chang et al., 2008). These were selected as the most appropriate variables to evidence if net hip and ankle joint moments act in synergy during the downstroke (Fregly & Zajac, 1996). Coupling angles (γ_i) were calculated from hip-ankle moment diagrams (Figure 1) for each crank-cycle data point for all revolutions of each participant's sprints (Chang et al., 2008). The coupling angle is defined as the orientation of the vector (relative to the right horizontal) between two adjacent points on the moment-moment plot, Figure 2. Since coupling angles are directional in nature, mean coupling angles were computed using circular statistics (Batschelet, 1981).

Mean coupling angles for each participant were categorised into four coordination phases: in-phase, anti-phase, hip-phase and ankle-phase, based on proposals of Chang et al. (2008) (Figure 2). When coupling angle values are 45° and 225° (a positive diagonal), components are in-phase: both hip and ankle moments are increasing or decreasing at similar rates, i.e., hip and ankle joints are working synergetically (Arnold et al., 2017). Conversely, when

coupling angles are 135° and 315° (a negative diagonal), components are anti-phase. For example, when hip moments are increasing, ankle moments are decreasing. When coupling angles are parallel to the horizontal (0° and 180°), ankle moments are changing, but not hip moments – ankle-phase. When coupling angles are parallel to the vertical (90° and 270°), hip moments are changing, but not ankle moments – hip-phase. Since coupling angles rarely lie precisely on these angles, the unit circle was split into 45° bins used by Chang et al. (2008) (Figure 2). Frequencies within which mean coupling angles lay in these coordination patterns, during the downstroke (defined between crank angles of 0 to 180°) were calculated for each participant, using the following equation: Frequency of coordination phase (%) = (Number of occurrences of coordination phase/51) × 100, (note there are 51 data points in the downstroke). This process was repeated to calculate group mean coupling angles for sprints at 135 rpm (Figure 3). Strength of hip-ankle synergies were quantified by the frequency of in-phase coordination pattern between hip and ankle moments in downstrokes.

2.5 Statistical analysis

Differences between frequencies of coordination phases were assessed using a Friedman test, with post-hoc Wilcoxon matched pairs using IBM SPSS Statistics Version 28 (IBM UK Ltd, Portsmouth, UK).

3 Results

Average left crank power over a complete revolution for sprints at 135 rpm was 494.1 ± 91.2 W. Hip and ankle moments were in-phase for 28.8% of the downstroke, with the hip-phase the most frequent coordination phase (42.5%) (Figure 4). A Friedman test ($\chi^2 = 19.3$, $P < 0.0005$) indicated that coordination phase frequencies differed across the four coordination phases. Post-hoc Wilcoxon matched pairs indicated that in-phase was significantly different

to anti-phase ($P = 0.004$), hip-phase ($P = 0.044$) and ankle phase ($P = 0.017$). Hip phases significantly differed to anti-phases ($P < 0.001$), and ankle phases ($P = 0.004$).

4 Discussion

We demonstrated that a vector coding method can be used to quantify strength of hip-ankle joint moment synergies during downstrokes in cycling. Data imply a tendency for hip and ankle joints to work in synergy in the downstroke during short-term maximal cycling at a pedalling rate of 135 rpm.

Findings revealing a weak synergy between hip and ankle joints in downstrokes at 135 rpm, support conclusions of simulation studies suggesting that hip and ankle joints need to work in synergy to transfer energy produced by hip extensors to the crank (Fregly & Zajac, 1996; Raasch et al., 1997). Fregly and Zajac (1996) modelled steady state pedalling at 75 rpm and Raasch et al. (1997) modelled the acceleration phase with pedalling rate increasing from 80 to 120 rpm through a revolution. Our results suggest that hip-ankle synergies may not be as strong at pedalling rates higher than previously modelled. The strength of hip-ankle synergies depend on time available in downstrokes to coordinate joint actions. At 75 rpm downstrokes last 0.40 seconds (pedalling rate used in Fregly and Zajac (1996) study), compared to 0.22 seconds at 135 rpm. The suggestion is that, as task complexity increases (e.g., due to changes in pedalling rate from 75 to 135 rpm), strength of hip-ankle synergies reduce, implying it is more challenging to coordinate joint moments at higher pedalling rates. This observation supports previous findings suggesting that, as task complexity increases, differences in coordination and coordination variability emerge (Weir et al., 2019).

At a pedalling rate of 135 rpm, the hip-phase is the most frequent coordination phase in downstrokes, suggesting that sprints at 135 rpm display a hip-dominant coordination pattern.

A much greater contribution from hip extension power to crank power at higher pedalling rates has been observed, proposing an optimal pedalling rate for maximum hip extension power at around 150 rpm, whereas the optimal pedalling rate for knee extension and flexion power was lower (McDaniel et al., 2014). Our finding that hip-phase coordination is dominant at higher pedalling rates elaborates on the notion that the role of the hip becomes more important at higher pedalling rates, from a power production and coordination perspective.

This study demonstrated the application of vector coding to quantify hip-ankle moment synergies in maximal cycling. Further research is required to investigate the presence of hip-ankle moment synergies in downstrokes at different pedalling rates and power outputs.

5 Conclusion

A modified vector coding technique can be used to quantify strength of hip-ankle moment synergies in cycling downstrokes. Hip and ankle joints tend to work in synergy in the downstroke during short-term maximal cycling, supporting findings of previous cycling simulation studies, highlighting it as a key biomechanical feature of maximal cycling. Data suggest that this method could be used to assess cyclists' pedalling techniques and to monitor effects of training or equipment interventions on coordination patterns.

6 References

- Arnold, J. B., Caravaggi, P., Fraysse, F., Thewlis, D., & Leardini, A. (2017). Movement coordination patterns between the foot joints during walking. *Journal of foot and ankle research*, 10(1), 1-7.
- Batschelet, E. (1981). *Circular statistics in biology*. Academic Press.

196 Bayne, H., Donaldson, B., Bezodis, N. (2020). *Inter-limb coordination during sprint*
197 *acceleration* 38th International Society of Biomechanics in Sport, Online, YouTube.

198 Burnie, L., Barratt, P., Davids, K., Worsfold, P., & Wheat, J. (2020). Biomechanical
199 measures of short-term maximal cycling on an ergometer: A test-retest study. *Sports*
200 *biomechanics*, 1-19. <https://doi.org/10.1080/14763141.2020.1773916>

201 Chang, R., Van Emmerik, R., & Hamill, J. (2008). Quantifying rearfoot–forefoot
202 coordination in human walking. *Journal of Biomechanics*, 41(14), 3101-3105.

203 de Leva, P. (1996). Adjustments to zatsiorsky-seluyanov's segment inertia parameters.
204 *Journal of Biomechanics*, 29(9), 1223-1230.

205 Dorel, S., Guilhem, G., Couturier, A., & Hug, F. (2012). Adjustment of muscle coordination
206 during an all-out sprint cycling task. *Medicine and science in sports and exercise*, 44(11),
207 2154-2164. <https://doi.org/10.1249/MSS.0b013e3182625423>

208 Dorel, S., Hautier, C. A., Rambaud, O., Rouffet, D., Praagh, E. V., Lacour, J. R., & Bourdin,
209 M. (2005). Torque and power-velocity relationships in cycling: Relevance to track sprint
210 performance in world-class cyclists. *International Journal of Sports Medicine*, 26(9), 739-
211 746. <https://doi.org/10.1055/s-2004-830493>

212 Elftman, H. (1939). Forces and energy changes in the leg during walking. *American journal*
213 *of physiology*, 125(2), 339-356.

214 Fregly, B. J., & Zajac, F. E. (1996). A state-space analysis of mechanical energy generation,
215 absorption, and transfer during pedaling. *Journal of Biomechanics*, 29(1), 81-90.

216 Hafer, J. F., Peacock, J., Zernicke, R. F., & Agresta, C. E. (2019). Segment coordination
217 variability differs by years of running experience. *Medicine and science in sports and*
218 *exercise*, 51(7), 1438-1443. <https://doi.org/10.1249/MSS.0000000000001913>

219 Hamill, J., Haddad, J. M., & McDermott, W. J. (2000). Issues in quantifying variability from
220 a dynamical systems perspective. *Journal of Applied Biomechanics*, 16(4), 407-418.

221 Kordi, A. M., Folland, J., Goodall, S., Menzies, C., Patel, T. S., Evans, M., Thomas, K., &
222 Howatson, G. (2020). Cycling-specific isometric resistance training improves peak power

output in elite sprint cyclists. *Scandinavian Journal of Medicine & Science in Sports*, 30, 1594-1604.

Martin, J. C., & Nichols, J. A. (2018). Simulated work loops predict maximal human cycling power. *Journal of Experimental Biology*, 221(13), jeb180109.
<https://doi.org/10.1242/jeb.180109>

McDaniel, J., Behjani, N. S. E. S. J., Brown, N. A. T., & Martin, J. C. (2014). Joint-specific power-pedaling rate relationships during maximal cycling. *Journal of Applied Biomechanics*, 30(3), 423-430.

Needham, R., Naemi, R., & Chockalingam, N. (2014). Quantifying lumbar–pelvis coordination during gait using a modified vector coding technique. *Journal of Biomechanics*, 47(5), 1020-1026.

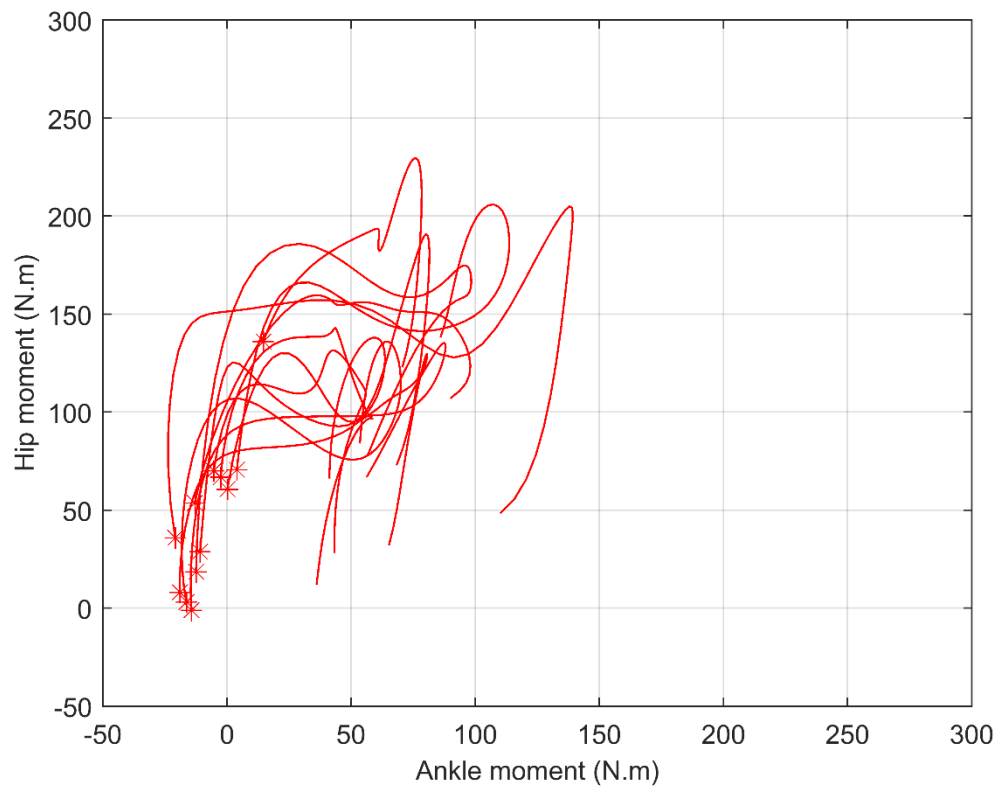
Raasch, C. C., Zajac, F. E., Ma, B., & Levine, W. S. (1997). Muscle coordination of maximum-speed pedaling. *Journal of Biomechanics*, 30(6), 595-602.
[https://doi.org/10.1016/S0021-9290\(96\)00188-1](https://doi.org/10.1016/S0021-9290(96)00188-1)

van Ingen Schenau, G. J., Boots, P. J. M., De Groot, G., Snackers, R. J., & van Woensel, W. W. L. M. (1992). The constrained control of force and position in multi-joint movements. *Neuroscience*, 46(1), 197-207.

van Soest, A. J., & Casius, L. J. (2000). Which factors determine the optimal pedaling rate in sprint cycling? *Medicine and science in sports and exercise*, 32(11), 1927-1934.

Weir, G., van Emmerik, R., Jewell, C., & Hamill, J. (2019). Coordination and variability during anticipated and unanticipated sidestepping. *Gait & posture*, 67, 1-8.

Wheat, J., & Glazier, P. S. (2006). Chapter 9: Measuring coordination and variability in coordination. In K. Davids, S. Bennett, & K. M. Newell (Eds.), *Movement system variability* (pp. 167-181). Human Kinetics.



249

250 **Figure 1: Mean hip-ankle moment plots for sprints at 135 rpm for the downstroke for**
251 **each participant, with * indicating top dead centre (TDC).**

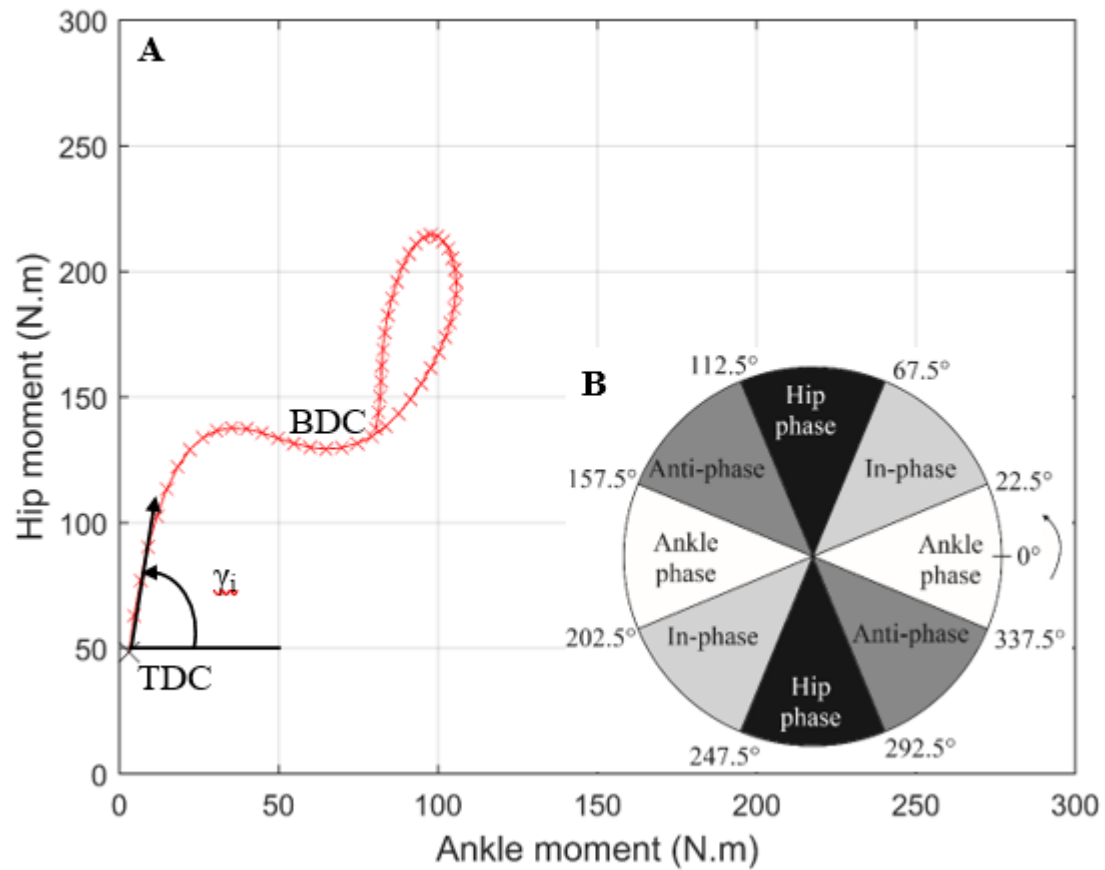


Figure 2: A: An illustration of the calculation for a coupling angle (γ_i) from hip-ankle moment plot (one downstroke during a sprint). Top dead centre (TDC) = 0°, and bottom dead centre (BDC) = 180°. B: The coordination pattern classification system for the coupling angle (γ_i)

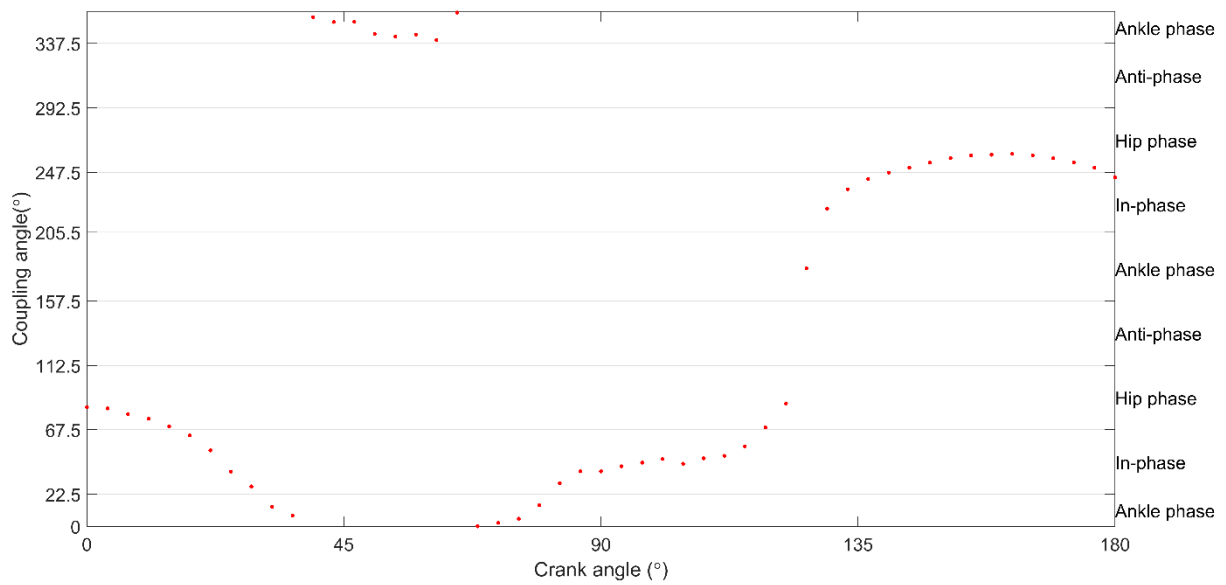


Figure 3: Mean coupling angle for hip-ankle moments for sprints at 135 rpm for the downstroke.

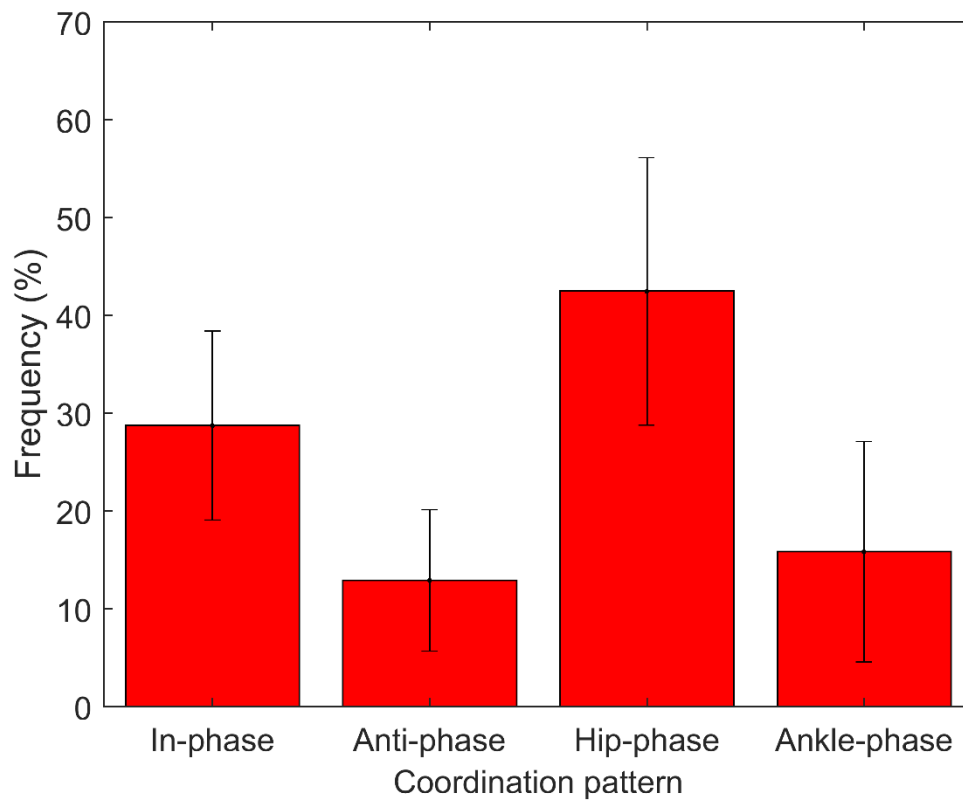


Figure 4: Hip-ankle moment coordination patterns during downstroke phase of the crank cycle for sprints at 135 rpm.